

The evolution of lithium in FGK dwarf stars

The Li rotation connection and the Li desert

F. Llorente de Andrés^{1,2,*}, C. Chavero³, R. de la Reza⁴, S. Roca-Fàbrega⁵ and C. Cifuentes²

¹ Ateneo de Almagro, Sección de Ciencia y Tecnología, 13270 Almagro, Spain

² Departamento de Astrofísica, Centro de Astrobiología (CAB, CSIC-INTA), ESAC Campus, Camino Bajo del Castillo s/n, 28692 Villanueva de la Cañada, Madrid, Spain

³ Observatorio Astronómico de Córdoba, Universidad Nacional de Córdoba, Laprida 854, 5000 Córdoba, CONICET, Argentina

⁴ Observatório Nacional, Rua General José Cristino 77, 28921-400 São Cristóvão, Rio de Janeiro, RJ, Brasil

⁵ Departamento de Física de la Tierra y Astrofísica and IPARCOS, Facultad de Ciencias Físicas, Plaza Ciencias, 1, Madrid, E-28040, Spain

Accepted 12 August 2021

ABSTRACT

We investigate two topics regarding solar mass FGK-type stars, the lithium rotation connection (LRC) and the existence of the “lithium desert”. We determine the minimum critical rotation velocity ($v \sin i$) related with the LRC separating slow from rapid stellar rotators, as being 5 km s^{-1} . This value also split different stellar properties. For the first time we explore the behaviour of the LRC for some stellar associations with ages between 45 Myr and 120 Myr. This allows us to study the LRC age dependence at the beginning of the general spin down stage for low mass stars, which starts at $\sim 30\text{--}40$ Myr. We find that each stellar group presents a characteristic minimum lithium (Li) depletion connected to a specific large rotation velocity and that this minimum changes with age. For instance, this minimum changes from $\sim 50 \text{ km s}^{-1}$ to less than 20 km s^{-1} in 200 Myr. Regarding the lithium desert, it was described as a limited region in the $A(\text{Li})\text{--}T_{\text{eff}}$ map containing no stars. Using T_{eff} from *Gaia* DR2 we detect 30 stars inside and/or near the same box defined originally as the Li desert. Due to their intrinsic T_{eff} errors some of these stars may be inside or outside the box, implying a large probability that the box contains several stars. Considering this last fact the “lithium desert” appears to be more a statistical distribution fluctuation than a real problem.

Key words. Stars: rotation – Stars: solar-type – Stars: abundances

1. Introduction

When the presence of the fragile atom of lithium (Li) was correctly detected and measured for the first time in the Sun by Müller, Peytremann & de La Reza (1975), a very important step was made towards the understanding of the stellar evolution of this element, ${}^7\text{Li}$ isotope. In fact, all this evolution reflects the history of the destruction of the original lithium, with which stars were born from the interstellar matter. The Li abundance, $A(\text{Li})$, of the interstellar medium depends on metallicity (Lambert & Reddy 2004; Lyubimkov 2016; Guiglion, et al. 2019). In view of this, we adopted the value of $A(\text{Li}) = 3.2 \pm 0.1^1$, which is also compatible with the meteoritic value of $A(\text{Li}) = 3.26 \pm 0.05$ (Asplund et al. 2009).

Stars, especially those with FGK-types and with masses near the Solar mass, which are our concern in this work, show two different stages of the Li depletion in their atmospheres. The first one happens during the rapid pre-main sequence (hereafter PMS) phase, in which a circumstellar disk is magnetically connected to the stellar surface, producing a halt of the stellar rotation. Because of this, a rapid initial Li depletion occurs, in an internal region between the base of the external convective zone (hereafter CZ) and the radiative stellar core. Here,

an important mixing is installed (see for instance the model of Eggenberger, et al. 2012).

Chavero, et al. (2019) applied this model to solar mass FGK-type stars, finding that with an initial original $A(\text{Li})$ of ~ 3.2 , depleted values were obtained of the order of $A(\text{Li}) \sim 2.0$ in a time scale of ~ 9 Myr, which is the lifetime of the protoplanetary disks, before stars enter into the main-sequence (hereafter MS) stage. During this last evolutionary phase, with a long lifetime scale of the order of 9–10 Gyr, a very slow and not well known physically Li depletion mechanism enters into action (see for instance Dumont et al. 2020). This slow depletion action was first proposed by Herbig (1966). Nevertheless, rapid stellar rotations can interfere on the Li depletion process. This is specially the case of the younger stellar groups, where rapid rotators are present. An important difference then appears, in which slow rotators are Li-poor and rapid rotators are Li-rich.

This property, which is part of the present study, is known in the literature as the “lithium-rotation connection” (hereafter LRC). Since the seminal study of this effect in the Sun by Conti (1968), the LRC mechanism has been the subject of several works. Contrary to some ideas that considered that a rapid stellar rotator will induce a strong internal mixing destroying Li, works by Butler et al. (1987) in the Pleiades open cluster (hereafter OC) with an age of ~ 125 Myr and in Alpha Per (50–70 Myr) by Balachandran, Lambert, & Stauffer (1988), showed that largest rotations preserve the Li. Soderblom et al. (1993) performed an

* fllorente@cab.inta-csic.es

¹ $A(\text{Li}) = \log[N(\text{Li})/N(\text{H})] + 12$

extended research of the LRC in the Pleiades, which was after revisited by King, Krishnamurthi, & Pinsonneault (2000) and recently by Barrado et al. (2016) and Bouvier et al. (2018).

These works confirmed and amplified the results of Soderblom et al. (1993). Another recent work by Arancibia et al. (2020) found that LRC is also present in a different type of stellar group, as the stellar stream Pec-Eri, with a similar age to the Pleiades. In this context a recent important analysis in the OC M35 (~ 150 Myr) has been presented recently by Jeffries et al. (2020). Is the LRC a universal property in the sense that LCR is present at different ages and in different kind of stellar groups? The LRC is present, for example, in NGC 2264, a very young OC with an age of 5 Myr (Bouvier et al. 2016), and its presence continues up to ages similar that of the Pleiades. A recent work have found indications of the presence of the LRC in an even younger OC (σ Ori) with an age of 3 Myr (Garcia 2021).

We note that the LCR it is also observed in different stellar young moving groups or associations (da Silva, et al. 2009; Messina et al. 2016). Several theoretical mechanisms have been proposed to explain the LRC property. In general these mechanisms involve the interaction between the base of the CZ and the hot internal burning region, where Li is destroyed. These studies regard a very slow diffusion acting in this intermediate zone (Rüdiger & Pipin 2001; Tschäpe & Rüdiger 2001). Other works are related to the action of penetrative convective plumes (Siess & Livio 1997; Baraffe, et al. 2017). Different mechanisms have also been invoked consisting on the reduction of the temperature at the base of the CZ produced by atmospheric inflation processes (Somers & Pinsonneault 2014; Somers & Stassun 2017). For a recent complete review on the action of the LRC see Bouvier (2020).

In the present study, we first propose to determine observationally the presence of a critical minimal velocity separating slow and rapid rotators, as is discussed in Baraffe, et al. (2017). Another aspect that we also consider here, consists on studying the LRC behaviour in stellar associations just after the beginning of the general spin down process era for solar mass stars, which happens at 30–40 Myr, (see, for instance, Bouvier et al. 2014). For this, we consider three stellar moving group candidates with a similar age of ~ 45 Myr which are: the Tucana-Horologium association (hereafter THA), the Columba association (COA) and the Carina association (CAA) (da Silva, et al. 2009). After, we consider the AB Doradus association (ABDA) with an age of ~ 120 Myr with a similar age as the Pleiades OC with an age of 125 My (Bell, Mamajek, & Naylor 2015; Bouvier et al. 2018).

Separately from the above described research within the present work, we tackle another different research, referring to the existence or not, of what is called the “lithium desert” (Ramírez, et al. 2012; Aguilera-Gómez, Ramírez & Chanamé 2018). This consists on a peculiar zone placed in the general A(Li) versus effective temperatures T_{eff} map, in which apparently no stars are found.

Our work is based in a sample of 1307 field MS stars of F5 to K4 spectral types, where 244 stars contain known planets, and 1063 stars, a priori without planets. Also, we consider 265 and 151 stars belonging to 14 OC and 4 associations, respectively. We have measurements of the Li abundances for all the mentioned objects with data obtained in the literature.

The stars chosen in this work are “non Li-Be-B Dip” stars whose mechanisms of depletion, especially for Li, are related to the shallow convection layers of these early-mid F-type stars acting in the above mentioned temperature interval (see for instance the model of Stephens, et al. 1997). By avoiding these early-mid F-type stars we are then considering, in general, stellar FGK ob-

jects with relatively small masses and relative large convective layers appropriate for a deep Li depletion acting mechanism, with stellar masses less than $1.5 M_{\odot}$ (Pinheiro, et al. 2014).

This work is the second of a series devoted to the study of Li which started with Chavero, et al. (2019). This paper is organised as follows: Section 2 presents the stellar data. Section 3 is centered on the study of the lithium-rotation connection. In Section 4 we address the problem of the existence or not of the so called “lithium desert”. Finally, we discuss and comment the conclusions in Section 5.

2. Data Collection

2.1. Sample of field stars

The origin of our current sample of field stars, listed in Table 1, is our previous work, Chavero, et al. (2019). From this first set we increase the number of objects in the sample looking for stars with Li measurements taken with a similar methodology, and all of them come from internally consistent ones. The search was carried out by means of using the Spanish Virtual Observatory (SVO) tool called `VOMultiCatalog_Interface`². It looks for the demanded stellar data by scanning all the catalogues within VizieR. In the case of lithium abundance, A(Li), we get information from about 11 catalogues (all references are displayed in Table 1). Once the stars have been identified, we proceed to triage them, as explained later.

In order to avoid any bias, we selected our stars without regard to their age, metallicity, rotational velocity or any previous detection (either dust nor planets). Just to detect if there is any influence by the presence of planets, in this work we take into account stars containing planets and those for which no planets have been detected. We proceeded this way since several studies presented evidence that the planetary formation process can modify the lithium of the host star (Israelian et al. 2004; Takeda & Kawanomoto 2005; Gonzalez, Carlson, & Tobin 2010). The nature of this disk-planet interaction will be object of study in another article.

A restrictive criterion that was imposed for the selection of the stars in the sample was, in addition to known A(Li), that the spectral types were FGK-type stars and whose masses were $M_{\star} < 1.5 M_{\odot}$. We thus eliminated, from the first sample, giant and subgiant stars. We found more than 2000 stars with reliable A(Li) values, but we dismissed this number of stars because we introduced a cut off in age at 10.5 Gyr. This cut is in order to eliminate the most evolved stars.

The final sample of Li abundances includes stars from the next 11 catalogues: Chavero, et al. (2019) as well as Aguilera-Gómez, Ramírez & Chanamé (2018); Bensby & Lind (2018); Cutispoto, et al. (2002); Delgado Mena, et al. (2014); da Silva, et al. (2009); Ghezzi, et al. (2010); Gonzalez (2015); Luck (2017); Ramírez, et al. (2012); Thevenin (1998). These works were selected because their data are coming from internally consistent measurements. We solved the dilemma of finding values from different authors by prioritizing those from the most recent publication. In the case of being our measured values from Chavero, et al. (2019) these were chosen in any case. For the corresponding stellar physical parameters, described below, we sought the greatest homogeneity among the different sources from which the data were collected.

The values of T_{eff} , without any restriction or cut both upper and lower, and parallaxes, were obtained from

² <http://svo2.cab.inta-csic.es>

the *Gaia* DR2 catalogue (Gaia Collaboration, et al. 2016; Gaia Collaboration et al. 2018). It gives uncertainty values for the effective temperature in terms of lower ($b_{T_{\text{eff}}}$) and upper limits ($B_{T_{\text{eff}}}$), terms in which T_{eff} values appear in the *Gaia* DR2 catalogue. All our stars belong to the “clean” subsample of T_{eff} recommended by Andrae, et al. (2018). We obtained the values of $[\text{Fe}/\text{H}]$ from Gaspar, Rieke & Ballering (2016) and Soubiran & Militzer (2016). V magnitude values were collected from the SIMBAD database. The search of $v \sin i$ implied searching within 30 catalogues. In this case we established as a priority the values published by Brewer, et al. (2016), and Delgado Mena, et al. (2015). In the case of not finding this value in the most recent works, we took them from the catalogue of Glebocki & Gnacinski (2005). All the catalogues from which the data have been obtained are listed in Table 1, along their respective references.

The age values have been obtained from 29 catalogues (see Table 1), in such a case we prioritised the more recent values, usually Delgado Mena, et al. (2019). However, this age scale might introduce inhomogeneities. Thus, for achieving greater homogeneity and for consistency with our previous work, we chose to derive ages and other evolutionary parameters, such as masses and radii, by using the PARAM 1.3 code (da Silva, et al. 2006). This code requires T_{eff} , $[\text{Fe}/\text{H}]$, V magnitude and parallax. So we have two sources for the age and the mass: one that comes from the literature, as described above, and the other from this work using PARAM³.

As mentioned in the introduction, this work is part of a set of them dedicated to the study of Li, which led us to complete the physical characteristics of our sample with the values of chromospheric activity index, $\log R'_{\text{HK}}$, which were mainly collected from Boro Saikia et al. (2018). When we did not find values in this catalogue we looked for them in Krejčová & Budaj (2012). In the first case, there are compiled 4454 stars, whose chromospheric activity was collected from a set of different sources. Such catalogue served to study the behaviour of the variation in the chromospheric activity of cool stars along the main sequence. The catalogue of Boro Saikia et al. (2018) listed different values for some stars. In such a case, we catalogued the average value and, as the error, the difference between the maximum and the minimum value. Also, using *Gaia* DR2 parallaxes, proper motions and radial velocities, and using the public software package PyGaia⁴, we obtained the galactocentric velocities U , V , W for all stars in our main catalogue. These last kinematic parameters plus the chromospheric activity are included in the sample to be used in a parallel work.

An additional observation is that, even within the giant planet regime, binaries tighter than 100 au show a different distribution of masses, suggesting a different formation mechanism and/or dynamical history (Duchêne 2010). In view of all these studies, we excluded from our samples 96 binary systems with semi-major axis $a < 100$ au to avoid introducing any bias in our analysis. Table 1 displays all these physical parameters and characteristics of our field sample stars with their respective reference.

Our catalogue is similar to that published by Aguilera-Gómez, Ramírez & Chanamé (2018) (hereafter AG18), but there are some differences whose consequences yield to different conclusions. So that, in order to guarantee that our data are as consistent as those already published, we

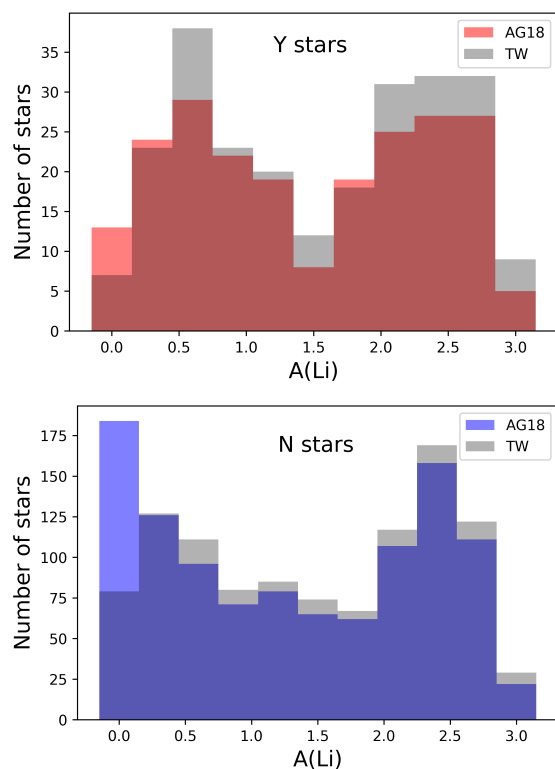


Fig. 1. Statistical distribution of the sample according to the star categorisation. The histograms built from both distributions, this work (TW) and AG18, for stars with (Y) and without (N) detected planets.

compared them with those published by AG18, because they normalise and homogenise their final catalogue. These authors divide in stars with (yes) and without (no) planets. In our case, we call *Y* stars to those with planets and *N* stars to those without planets. We should know that the AG18 catalogue is bigger than ours because it is a complete catalogue of 2318 stars, which 1470 of them are categorised in stars with or without planets. The main difference between their catalogue and ours is the number of stars with planets (213 and 244 stars with planets, respectively), and without planets (980 and 1063 respectively). The mentioned difference comes from the fact that, in the sample of AG18 some stars are listed but without mention if they host planets or not. We did not take them into account. They are not useful for our objectives. Moreover AG18’s sample contains a mixture of giants, sub-giants and dwarfs. In a parallel work we have already seen that the distribution of Li in giants and dwarfs is practically the same, exception made for some Li rich giants. This mixture is responsible for the difference that shows the intercept value that in the equation that relates the temperature of our sample with the sample of AG18.

Next are the relations between Li, $[\text{Fe}/\text{H}]$, T_{eff} and age of this present work (TW) with respect to AG18 listed values:

$$A(\text{Li})_{\text{TW}} = 0.99A(\text{Li})_{\text{AG18}} + 0.01, R^2 = 0.99$$

$$[\text{Fe}/\text{H}]_{\text{TW}} = 0.99[\text{Fe}/\text{H}]_{\text{AG18}} + 0.001, R^2 = 0.99$$

$$T_{\text{eff TW}} = 0.93T_{\text{eff AG18}} + 397, R^2 = 0.88$$

$$\text{Age}_{\text{TW}} = 0.88\text{Age}_{\text{AG18}} + 0.33, R^2 = 0.81$$

The relations are similar, the big difference is in the number of stars with $v \sin i$ known: in AG18 sample, stars with planets

³ http://stev.oapd.inaf.it/cgi-bin/param_1.3

⁴ <http://https://github.com/agabrown/PyGaia>

Table 1. Stellar parameters of the sample

Star	SpType	T_{eff} (K)	M_{\star} (M_{\odot})	[Fe/H] (dex)	A(Li)	$v \sin i$ (km s^{-1})	Age(P) (Gyr)	Age(L) (Gyr)	$\log R'_{HK}$	U V W (km s^{-1})	PI
HD1461	G5V	5764 ± 81	1.06 ± 0.03	0.19 ± 0.01^a	0.6 ± 0.07^A	1.8^1	3.1 ± 2.3	5.6 ± 1.5^3	-5.14 ± 0.18^4	-31.74, -38.86, -1.62	Y
HD1832	G2/3V	5773 ± 74	0.98 ± 0.03	-0.03 ± 0.03^a	1.08 ± 0.07^B	2.8 ± 0.5^2	7.3 ± 2.4	8.5 ± 1.4^3	-4.64 ± -0.15^4	-7.27, -62.72, -16.94	N
...											

References. (1) Col.1: Henry-Draper catalogue name; Col.2: spectral type; Col.3: effective temperature taken from *Gaia* DR2 where the uncertainty is taken as $(B_{T_{\text{eff}}} - b_{T_{\text{eff}}})/2$; Col.4 stellar mass calculated using PARAM code; Col.5: stellar metallicity, (a) Gaspar, Rieke & Ballering (2016); Col.6: lithium abundance, (A) Chavero, et al. (2019), (B) Aguilera-Gómez, Ramírez & Chanamé (2018); Col.7: projected rotational velocity, (1) Brewer, et al. (2016), (2) Marsden, et al. (2014) Col.8: stellar age calculated using PARAM code; Col.9: stellar age taken from literature, (3) Aguilera-Gómez, Ramírez & Chanamé (2018); Col.10: chromospheric activity index, (4) Boro Saikia et al. (2018); Col.11: presence of planet Yes or No; Col.12: galactocentric velocities U, V, W. Full Table 1 and references are only available in electronic format at the CDS via.

115 with $v \sin i$, against 245 stars in our sample; in the case of stars without planets, the sample of AG18 contains 358, against to 931 in our sample. The two samples, AG18 and ours, show the same statistical distribution of the lithium abundance, even grouping into stars with and without planets and the total sample size (see Figure 1).

2.2. Sample of open cluster stars

To be able to have more references in terms of stars with high rotation speeds, we include stars of open clusters with an abundance of known Li that also allows us to have a larger sample of stars younger than 300 Myr. The aim is to establish a reference (Table 2) constructed with the cluster data that, in addition to the stellar sample (Table 1), help us to explain our results. The first source of data comes from the stars with Li abundances identified in the literature and belonging to open clusters, collected by Sestito & Randich (2005) and published in WEBDA⁵. We added data of the OCs NGC6253 (Cummings, et al. 2012) and NGC3680 (Anthony-Twarog, et al. 2009) in order to increase the age range of cluster stars within the same range of T_{eff} and surface gravity ($\log g$) that means MS stars. Ages were taken mainly from Kharchenko, et al. (2013).

In the present study we assume uniform Li abundance in a cluster before any Li depletion occurs. But, to zeroth order, the initial Li of near-solar-metallicity open clusters should be similar to the meteoritic abundance. This A(Li) value is observed in very-young open clusters, which are generally in the range of $A(\text{Li}) = 3.0$ to 3.4 . We assumed that for the normal stars of the youngest cluster NGC 2264, plenty of T-Tauri stars, do not present Li depletion.

Table 2 contains data of the OCs and also young stellar associations that have been considered in this work. We have performed a deep probabilistic study to ensure that each cluster star is member of their host cluster. The membership is based upon probability following and applying the criteria quoted from Kharchenko, et al. (2013) and Dias et al. (2014). So that a star is membership of its host cluster if its probability of belonging to it is around 61% in the Dias catalogue and stars with kinematic and photometric membership probabilities higher than 60% in the Karchenko one. With these crossed restrictions, we admit that our selected stars are members of their respective host clusters, with a high probability of at least 90%.

We checked if the cluster stars are MS stars or not, by means of the colour-magnitude diagram (CMD) of every cluster. We conclude and confirm from all these CMD diagrams that all our

⁵ WEBDA database is operated at the Department of Theoretical Physics and Astrophysics of the Masaryk University.

Table 2. Parameters of stars in Open Clusters and Stellar Associations

Cluster	Star	$v \sin i$ (km s^{-1})	A(Li)	T_{eff} (K)
IC 2602	IC 2602 120	51.2	3.19	5650
Age=0.037 Gyr	IC 2602 131	45.7	3.06	6147
(c)	IC 2602 132	14.7	2.98	6041
	IC 2602 157	11.8	2.92	5624
	IC 2602 2290	19.2	1.76	4553
	IC 2602 2830	30	3.22	5746
	IC 2602 2951	10.9	3.00	5190
...

References. (c) Heiter et al. (2014). Full version of the Table and references are only available in electronic format at the CDS via.

sample cluster stars belong to the MS with $4000 \text{ K} < T_{\text{eff}} < 6500 \text{ K}$. Stellar parameters of cluster stars, such as effective temperature, T_{eff} , projected rotational velocity, $v \sin i$, stellar mass, M_{\star} , and metallicities, [Fe/H], were collected from the literature. Exceptionally, when a T_{eff} value was not found we quoted the one listed in WEBDA. The literature values are collected by means of VOMultiCatalog-Interface. The sample of cluster stars and their parameters is large enough to explore how the lithium abundance, A(Li), behaves in stars belonging to OCs.

The total number of remaining OC stars being part of this study is 265 objects. Their spectral types are mainly F, G and K type stars. Although the listed values of A(Li) were computed assuming LTE (local thermodynamic equilibrium) and NLTE (non-local thermodynamic equilibrium), our study is based in general on the NLTE assumption. All the clusters and stars data are listed in Table 2, which contains, for each OC/Association: identification, age in Gyr, star name, $v \sin i$ in km s^{-1} , Li abundance and effective temperature T_{eff} in K.

2.3. Sample of young stellar associations

We consider four stellar associations and studied for the first time the LRC process (see Table 2) in stars with stellar effective temperature $T_{\text{eff}} > 4000 \text{ K}$. These are three moving groups with a similar age of $\sim 45 \text{ Myr}$, Tucana-Horologium, Columba and Carina associations and a fourth one, the AB Doradus association with an age of $\sim 120 \text{ Myr}$ (da Silva, et al. 2009). Thus the sample (field stars and OC stars) is widened by the addition of 167 stars of young stellar associations.

We also compare this last group to the OC Pleiades (125 Myr) because these two stellar groups are considered to have a common origin (Luhman, Stauffer, & Mamajek 2005;

Ortega et al. 2007) and they also have a similar age. These studies permit us to see the evolution of the LRC first in an age interval of near 100 Myr.

This study requires a careful examination of which of the published members of these associations are to be considered as intruder members. In principle, there are two methods to detect them and these are made by means of Galactic dynamics or by a chemical abundance analysis. In the dynamical method, the 3D orbits of all the members of a moving group follow dynamical trajectories from an initial point considered to be the origin of the association in the past, up to the present observed positions. These orbits are established by the action of a general Galactic potential. Any interloper is easily detected because its orbit follows a very different trajectory from all the members of the group. In the dynamical method used by Ortega et al. (2007), used to determine the origin of ABDA from the Pleiades, any interloper member has been detected. Nevertheless, a chemical analysis by Barenfeld et al. (2013) of ABDA, suggested that some members of what they call the stream, in contrast to the “nucleus” of ABDA, contain certain suspicious chemical members. In any case, the metallicity determined by Ortega et al. (2007) is compatible with that obtained by Barenfeld et al. (2013).

Translated into an intruder selection, we identified as a non-member, any star that has a specific individual metallicity value different by larger than a factor 0.1 dex from the mean metallicity representing that of the group. For this, we first estimate the mean metallicity ($[Fe/H]$) of each association by considering the ensemble of members presenting a homogenous distribution of metallicities. We are aware that these are new values in the sense that we have not found comparative values in the literature, with the exception of ABDA. The respective mean metallicities are: for THA the $[Fe/H] = -0.04$, for COA $[Fe/H] = 0.002$, for CAA $[Fe/H] = 0.02$ and for ABDA $[Fe/H] = 0.02$. For ABDA, we note that a more precise value for the metallicity obtained by Barenfeld et al. (2013) is equal to 0.02 ± 0.02 . The respective intruders are not considered in this work, and we identify them in the Figures with a black square symbol in each of the $A(Li)$ versus $v \sin i$ Figures presented and also marked in Table 2.

3. On the lithium-rotation connection

As mentioned in the introduction, the stellar rotation plays a very important role in the Li depletion during the PMS and MS evolutionary stages. When the projected rotational velocity is such that $v \sin i > v_{cr}$, where v_{cr} is a critical rotation velocity the stars inhibit somehow the Li depletion, appearing as Li-rich stars. Determining its critical value is the objective of this work. On the contrary, if the $v \sin i < v_{cr}$, it means below 5 s^{-1} , the stars appear as Li-poor stars. This is the case for the FGK-type stars with masses between $0.8\text{--}1.4 M_{\odot}$ considered in this work. There are very few exceptions that will be discussed below. This property represents the LRC as is defined in the introduction. In the precedent Sections 2.2 and 2.3 we discuss the contents of our data concerning the stellar open clusters and associations respectively.

Here, we discuss some of the main properties of field stars which represent a large part of our data. For this we present in Figure 2 a general map of the distribution of the Li abundances $A(Li)$ of field stars (being planet hosts or not) in function of T_{eff} (*Gaia* values). Also, a scale of their $v \sin i$ velocities is introduced in the Figure. The aim of Figure 2 is to show the three parameters involved together, this is: T_{eff} , $v \sin i$ and $A(Li)$ and to explore some indications of the presence of a global LRC effect and also of a $v \sin i$ critical value separating rapid and slow stel-

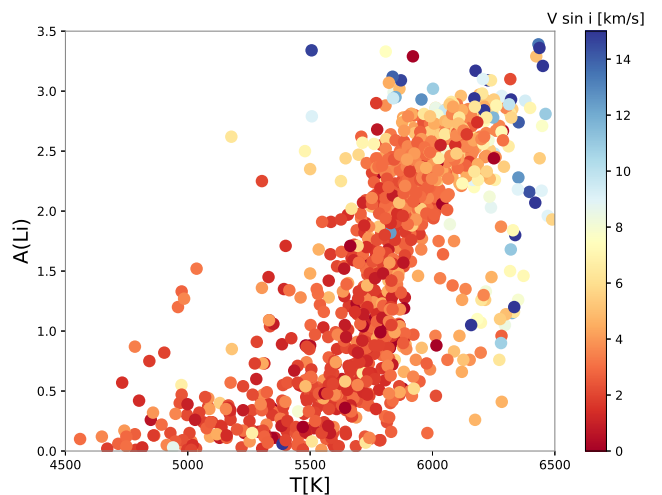


Fig. 2. Lithium abundance as a function of effective temperature for all stars in our catalog for our sample of field stars, where the color bar indicates the $v \sin i$ velocity in km s^{-1} . Whereas the general population is dominated by low rotating stars. One small group is represented by some rapid rotators at $T_{eff} > 6300 \text{ K}$ but with anomalous low $A(Li)$ values.

lar rotators. As seen, this Figure is dominated by the presence of slow rotators (blue points) which could be of different ages. Some medium and rapid stellar rotators (yellow and red points) at high T_{eff} values are also present, which eventually suggest the presence of a vague LRC effect. However, due to the complete mixture of ages among these field stars, and the presence of several slow rotators stars in the Li-rich region, no robust conclusion can be obtained. This is also the case with the determination of any critical velocity, even with the presence of very few stars (yellow points) with $v \sin i \approx 5 \text{ km s}^{-1}$. We conclude that the presence of the LRC and a critical $v \sin i$ must be studied using other methodology and this is the subject of the next sections.

Within the Figure 2 are distinguished stars that do not adhere to the general behaviour. Identify themselves by presenting the following characteristics: there are 4 stars (HD149724, HD16548, HD166 and HD211080) with $T_{eff} < 5700 \text{ K}$ and low rotation ($v \sin i < 5 \text{ km s}^{-1}$) but high abundance ($A(Li) > 2.0$). Their high abundance is explained by their high metallicity (average of $[Fe/H] = 0.22$) and high activity (average of $\log R'_{HK} \sim -4.54$ face to the mean value of -4.75) as described by Boro Saikia et al. (2018).

Additionally, in Figure 2 there are six stars of late F-type with $T_{eff} > 5700 \text{ K}$, and high rotation ($v \sin i > 8 \text{ km s}^{-1}$) but low abundance ($A(Li) < 1.5$), these are: HD107213, HD185720, HD201203, HD30736, HD53665 HD86264. The action of rotationally induced slow mixing can explain the low Li value as the result of slow Li mixing in these stars that are currently undergoing angular momentum loss and are sufficiently massive (their average mass $\sim 1.4 M_{\odot}$) that interior temperatures and densities are sufficiently large to burn Li as a result of such mixing (Baugh et al. 2013). More detailed conclusions on the critical velocity will be seen in Section 3.1. Also, many more properties on the LRC will be obtained with the help of stars of clusters and associations in Section 3.2.

3.1. The minimum critical rotational velocity of our complete sample stars

In this section we set out to obtain a numerical figure that is the actual physical value, both for field and cluster stars. Figure 2 guides us to visualise a value for critical rotational velocity, separating fast and slow rotating stars. Figure 3 shows the $A(\text{Li})$ as a function of the projected rotational velocity, $v \sin i$, colour-coding with the age and the effective temperature. We must note that the ages estimated for field stars (see Table 1) are much less precise than those of cluster ages (Table 2). We have not represented the masses on the third axis since we only have the values of these for the field stars, in doing so with the T_{eff} , we preserve homogeneity, while it is a way of representing the equivalent masses. In short, the identification of the critical rotational velocity involve also the other involved stellar parameters.

Our search for this critical $v \sin i$ rotational velocity, involves also the investigation of the effects of the physical parameters mentioned above. Our method was based on analysing the mosaic depicted in Figure 3. We first consider the case of the very slow rotational velocities with $v \sin i \leq 5 \text{ km s}^{-1}$. In Figure 3, for the whole lithium abundances ranging $A(\text{Li}) \sim 0.0$ up to 3.3, the field and cluster stars present a mixed collection of ages and T_{eff} values. This collection represents some different Li evolution scenarios. For field stars without planets (Figure 3 a, b) and with planets (Figure 3 c, d), we can distinguish two intervals of $A(\text{Li})$ bounded by the value of $A(\text{Li}) \sim 2.5$. In general, stars with $A(\text{Li}) < 2.5$ are cooler than $\sim 6000 \text{ K}$ and older than 4 Gyr. For the less numerous Li-rich stars with $A(\text{Li}) > 2.5$, these are younger than $\sim 3 \text{ Gyr}$ and hotter than 6000 K. We emphasise that this behaviour is similar for stars hosting or not planets. In the case of clusters (Figure 3e, f) the presence of quite very cool stars ($\sim 4500 \text{ K}$) is more accentuated for $A(\text{Li}) < 2.5$. For Li-rich stars with $A(\text{Li}) > 2.5$, stars appear to have temperatures of 6000 K or higher, with ages between $\sim 0.2 \text{ Gyr}$ and 0.6 Gyr. We must note that the separating value of the lithium abundance of 2.5, not only distinguish two different zones of age and temperatures as can be seen in Figure 3, but, remarkably, is similar to the upper limit of the final PMS depleted Li values between 2.2 and 2.4 as found in Chavero, et al. (2019).

We also examine the situation for larger rotational velocities ($v \sin i > 5 \text{ km s}^{-1}$) for field stars, hosting or not planets, and for those belonging to clusters. First of all, stars with $A(\text{Li}) > 2.5$ present, in all cases, a normal behaviour for the LRC phenomena. This means, for high rotation velocities, stars maintain in general their original lithium abundance. We note that cluster stars, differently from field stars, present very high rotational velocities as expected because some of them are younger than those of our field sample. What appears to be more peculiar in this case of larger velocities, is the presence of dispersed, relatively Li-poor stars with $A(\text{Li}) < 2.0$. This peculiarity is more notorious if we consider that the temperatures of field stars dispersed are different and opposite than those in clusters. Dispersed field stars are hot and cluster stars are cool. However, in both cases they are relatively young objects. This difference indicates different origins. In the following we try to explain these origins. We first consider the case of the OC.

A complete discussion on this is given in the next Subsection 3.2. Nevertheless, we can say that in OC, which occupy a large range of ages, their stars suffer after 30-40 Myr a general spin down effect (Bouvier et al. 2014). During this process, the cool K-type member stars are the first, in each cluster, to be Li depleted. In this way, from ages around 100 Myr and older ages, K-type dwarfs began to successively down to the low Li abun-

dance zone (see for example the case of the Pleiades OC with an age of 125 Myr in Fig. 5 (b)). The presence of the dispersed cool stars and relative young stars in clusters in Figure 3(e, f) is the result of this process.

The distribution of field stars as shown in Figure 3(a to d), requires a different explanation from that of the OC, this because their evolution differ from what we call, the general and standard Li depletion processes in solar type stars. As mentioned before, the most important Li depletion occurs in the initial T Tauri phase. Here, around 70 % of T Tauri stars (Armitage, Clarke, & Palla 2003) maintain their accretion disks with lifetimes up to 10 Myr. In the introduction we mentioned that using the accretion disk braking model of Eggenberger, et al. (2012), the Li abundances are reduced to $A(\text{Li})$ values near 2.0 (Chavero, et al. 2019).

In Figure 3 (a to d) two different zones appear to escape this standard Li depleting process. They are represented first, by few Li-rich objects, with low rotation velocities ($v \sin i \leq 5 \text{ km s}^{-1}$). The second group is formed by dispersed Li-poor objects with more larger velocities ($v \sin i > 5 \text{ km s}^{-1}$). These stars are hotter than 6000 K and younger than 4 Gyr. Summarising, these last mentioned two groups present mechanisms inverse to those acting in the standard Li process. Even if these two mentioned groups represent minor groups, they require eventual future, non standard physical explanations, which consider supplementary mechanisms in the complex disk-star interaction (Ireland et al. 2021). We presented an ensemble of different stellar properties, as age and temperatures (or mass equivalent) for stars with rotational velocities less or larger than $v \sin i = 5 \text{ km s}^{-1}$. Considering all these physical evidences, we can conclude that the velocity of $v \sin i$ of 5 km s^{-1} is the most representative critical rotational velocity to separate, not only slow and rapid stellar rotators, but also differentiated stellar properties

This determined critical value of $v \sin i$ is important in the light of models trying to explore the LRC mechanism. For instance Baraffe, et al. (2017) used for this a new diffusion mechanism by means of hydrodynamic simulations. They introduce an overshoot in the form of plumes at the lower edge of the CZ. Their results show that the stellar rotation affects the mixing in the CZ bottom. One of their main results, is the prediction of the existence of a critical rotation above which the rotation prevents the penetration of any plumes. In addition, below this critical velocity value, rotation has small or no effects, even in the case of most vigorous plumes.

3.2. The complete pattern of the lithium rotation connection

The representation of the variation of the $A(\text{Li})$ in function of rotational $v \sin i$ velocities for a stellar group (OC or association) is a very practical representation to distinguish changes in the behaviour of the Li depletion. The general pattern of the LRC is formed by two very different behaviours. On the one hand, by the presence of stars with very small $v \sin i$ values ($\leq 5 \text{ km s}^{-1}$) covering a wide range of the $A(\text{Li})$ depleted values, from the initial value of ~ 3.3 down to very depleted near zero values in some cases. It is generally considered that stars presenting this behaviour have braked their larger past rotations, for example by the PMS mechanism as mentioned in the introduction (Eggenberger, et al. 2012) and by a slowly Li depletion mechanism during the MS. On the other hand, a complete different behaviour appears when the projected rotational is over the initial threshold velocity of $\sim 5\text{-}10 \text{ km s}^{-1}$.

These stars appear to be less and less Li depleted. This pattern shows that the Li depletion is reduced progressively up to a

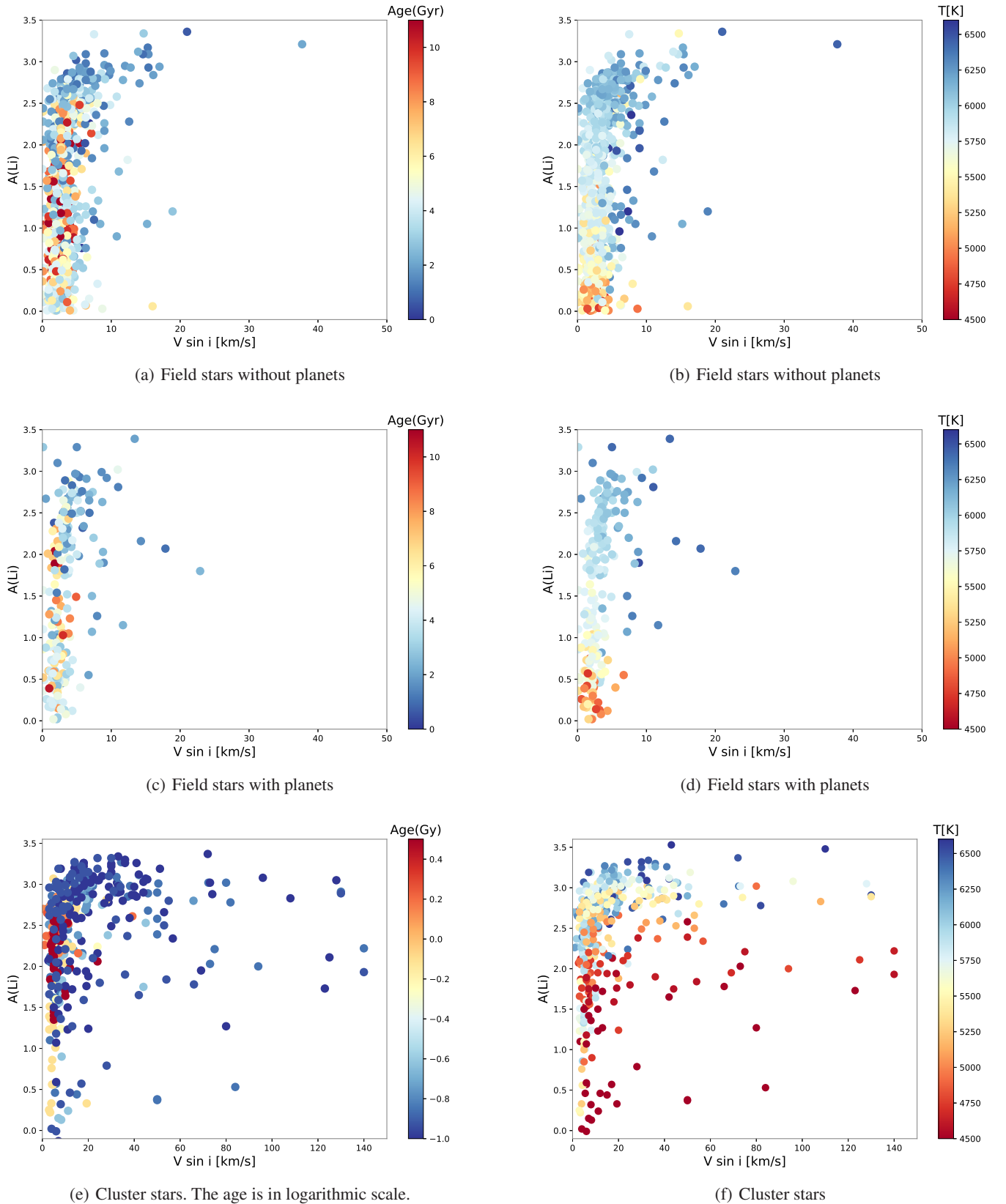


Fig. 3. $A(\text{Li})$ versus $v \sin i$. Points are colored according to the age (panels a, c, e) and the T_{eff} (panels b, d, f) of the stars as indicated by the color bar on the right of the graph. Panels (a) and (b) corresponding to field stars without detected planets, whereas panels (c) and (d) corresponding to field stars with detected planets. Cluster stars are represented in the panels (e) and (f). The diagram of panel e) shows the age in a logarithmic colour scale ranging from dark blue for 0.035 Gyr to red for 5 Gyr.

minimum stage. As we will see later, this specific minimum Li depletion changes with age. Let us reconsider and ask ourselves if the Li depletion for all large and very large rotational velocities continues to be constant or this one diminishes. Is this behaviour age dependent?

Thus Figure 3b shows that there are some speeds above 5 km s^{-1} at which the $A(\text{Li})$ reaches the primordial value to decrease for larger $v \sin i$ values. Not being able to know precisely what these critical speeds were, we decided to examine here the behaviour of the LRC action using young stellar moving groups or associations with different ages. These are: the Tucana-Horologium, the Columba and the Carina associations with a similar age of 45 Myr (da Silva, et al. 2009), and the AB Doradus association with an age of ~ 120 Myr (Bell, Mamajek, & Naylor 2015). We also examine the Pleiades OC.

The first indication of the presence of the LRC action for a representative number of moving groups or associations, can be found in da Silva, et al. (2009). This was made for an ensemble of nine associations which present different degrees of the LRC effect. However, no association has been studied in detail with the exception of the young (20 Myr) Beta Pic association (Messina et al. 2016). This last work was made by means of observed photometric periods detecting however, that the LRC effect appears to be more important, only for lower mass stars with masses in the interval of $0.3\text{--}0.8 M_{\odot}$.

3.2.1. The Tucana-Horologium, Columba and Carina associations

The stellar moving groups or associations THA, COA and CAA are sparse groups of stars located at distances between 35 and 160 pc. Each association is distinguishable by their similar space velocities in all of its components. Each association is considered to have a specific spatial formation region in an interstellar cloud, now vanished. It is from this original place of formation that all members began to move. The time elapsed since the considered epoch of formation and the time of the present observable positions, is one of the methods to obtain the age of the group. The discovery of THA has been made by Torres et al. (2000) and Zuckerman & Webb (2000), whereas the discovery of COA and CAA were made and discussed by Torres et al. (2008). The source of $A(\text{Li})$ and $v \sin i$ data to study the LRC for these three moving groups are taken from da Silva, et al. (2009). In Figure 4 we present the distribution of $A(\text{Li})$ in function of $v \sin i$ for the ensemble of these three associations having similar ages, by different colours. The internal errors of the $A(\text{Li})$ values have been discussed in da Silva, et al. (2009) and are in general less than a factor 0.2. In any case the internal errors will not modify in a significant way, the general distribution of points in Figure 4. The presented values of $A(\text{Li})$ and $v \sin i$ are then sufficient to reach our goal. The rotational velocities $v \sin i$ are projected velocities that do not represent always the true equatorial rotational velocities. Some considerations about these differences of velocities will be discussed later in Section 3.2.3.

The respective number of our detected intruders members in the lists of da Silva, et al. (2009) of these three associations are: THA (8 intruders), COA (3) and CAA (3). All these considered non-members are shown in Figure 4 marked with a black square overlapped to the different symbols corresponding to each association. We adopt here the ages of Bell, Mamajek, & Naylor (2015). Using a self-consistent isochronal scale they obtained the following ages for these three associations: THA (45 ± 4 Myr); COA (42^{+6}_{-4} Myr) and CAA (45^{+11}_{-7} Myr). For our compara-

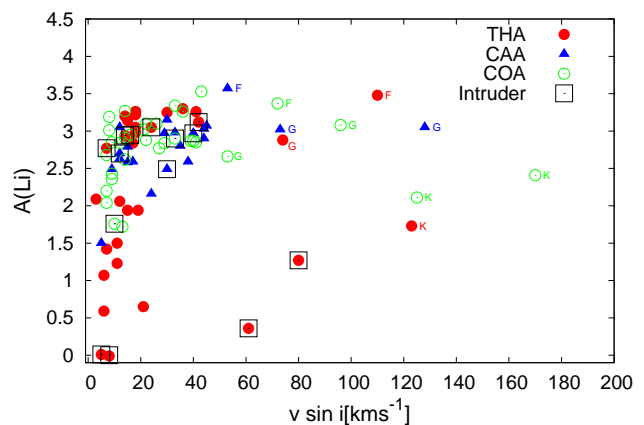


Fig. 4. $A(\text{Li})$ versus $v \sin i$ of genuine stars of the associations Tuc-Hor, Columba and Carina. Different symbols represent: red filled circles for Tuc-Hor, green open circles for Columba and blue filled triangles for Carina. Intruder stars not considered in this work, are shown with a black square overlapped to the different symbols. All $A(\text{Li})$ values are maintained as presented by the authors (da Silva, et al. 2009). The spectral types are marked for rapid stellar rotators.

tive analysis we consider a mean age equal to 45 Myr for all of them.

The distribution of points in Figure 4 representing the real considered members of THA, COA and CAA have the general typical pattern expected to reflect the LRC as mentioned before. The LRC is represented by stars showing highly Li depleted stars for $v \sin i < 10 \text{ km s}^{-1}$.

For larger $v \sin i$ velocities, an important feature appears in Figure 4. This is the presence of a minimum of the Li depletion corresponding to the rotational velocity of $v \sin i \sim 50 \text{ km s}^{-1}$. For even larger velocities, FG-type stars are distributed in an almost horizontal sequence. Contrary, K-type dwarf stars shown a much more important Li depletion for very rapid stellar rotators. As we explain in the next subsection, older stellar groups present different behaviours regarding this general stellar distribution of the LRC.

3.2.2. The AB Doradus association

The richest populated association ABDA is the most studied among the moving groups considered here. The literature gives a collection of different ages. They are in an increasing age scale from 50–70 Myr (Zuckerman, Song, & Bessell 2004; Torres et al. 2008; da Silva, et al. 2009) to a coeval age of 119 ± 20 Myr in Ortega et al. (2007). More recent age values for ABDA and lastly, that of Bell, Mamajek, & Naylor (2015), which gives an age of 149^{+51}_{-19} Myr. In order to study more in detail the common origin of ABDA and the Pleiades OC we compare the action of the LRC in both stellar groups. Figure 5a shows the distribution of $A(\text{Li})$ in function of $v \sin i$ velocities of stars of ABDA. Figure 5b presents the same distribution for stars in the Pleiades for which both values of the $v \sin i$ projected rotation velocities and the $A(\text{Li})$ values are took from Barrado et al. (2016). New features appear for these stellar structures, almost 100 Myr older than the previous three younger associations considered. In ABDA the minimum Li depletion appears at $v \sin i \sim 30 \text{ km s}^{-1}$, which is a smaller value than that of $\sim 50 \text{ km s}^{-1}$ of the 45 Myr associations. At this velocity, two branches of stars appear and instead of one branch as was the case for the younger

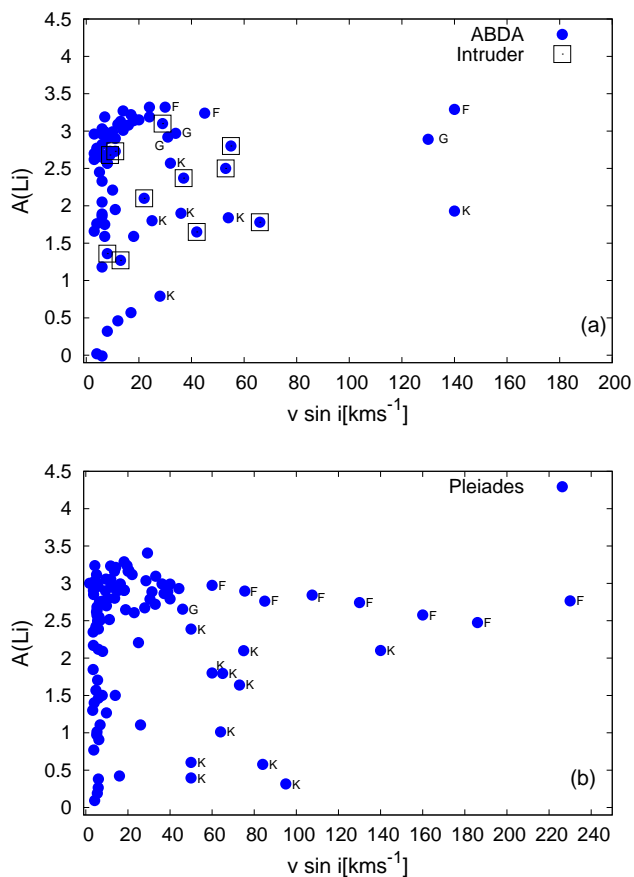


Fig. 5. Same representation as in Figure 4 for stars of the AB Dor association with an age of ~ 120 Myr (top panel a) and of the open cluster Pleiades with an age of 125 Myr (bottom panel b). As in Figure 4, the distribution shows that the few more Li depleted stars are K-dwarf stars. The spectral types are marked for stars with $v \sin i > 30$. Intruder stars in AB Dor are represented by open squares. Values of the Pleiades stars are taken from Barrado et al. (2016)

are those of Barenfeld et al. (2013), which established a minimum age of 110 Myr (Figure 4).

As it can be seen in both Figures 5a and 5b, the general pattern is similar. A first branch showing very strong Li depletions appears, specially for the case of the Pleiades. This branch initially formed appears at $v \sin i \sim 30 \text{ km s}^{-1}$ is then followed by very Li depleted stars, all of them represented by K-type dwarf stars. A second branch, almost horizontal, with much less Li depleted values appears, formed essentially by F-type stars. However, in this “horizontal” branch, some examples of rare, very fast rotators G and K-type stars are present, indicating a normal stratification of some Li depleted values. In the next sub-section we discuss more in detail this effect.

3.2.3. On the nature of some very rapid rotators in associations: Projected versus equatorial rotations velocities

An important work that helps to understand the effects of rotation in associations is that of Messina et al. (2010). For these associations they measured the photometric stellar rotation periods and, at the same time, they estimated the stellar radii by comparing the stars positions in a colour-magnitude diagram with evolutionary tracks. This data enabled them to calculate the equato-

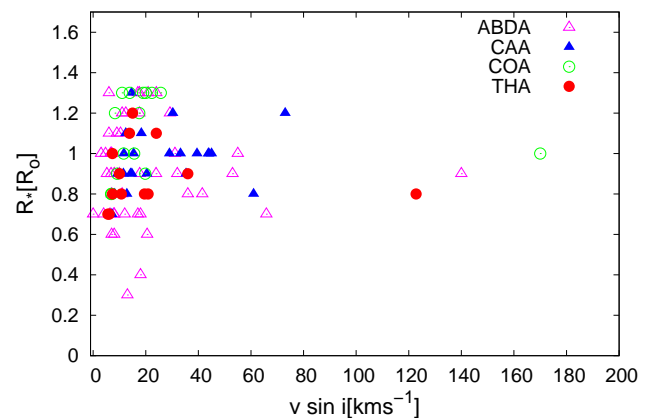


Fig. 6. Stellar radii versus $v \sin i$ for the associations Tuc-Hor, Columba, Carina and AB Dor. It can be seen that the radii of the more rapid rotators corresponds to the radii of K-type dwarf stars which are those presenting more Li depleted values.

rial rotation velocities for the individual stars as $\mathcal{V}_{eq} = 2\pi(R/P)$ where R is the stellar radius and P the rotation period. Figure 5 in Messina et al. (2010) represents a diagram of observed projected $v \sin i$ velocities versus the calculated and measured \mathcal{V}_{eq} velocities. It is interesting to note that in general, for $v \sin i$ or \mathcal{V}_{eq} values less than $\sim 50 \text{ km s}^{-1}$, a large part of the individual points pertaining to several associations, are placed near the diagonal defined by $v \sin i = \mathcal{V}_{eq}$, corresponding to equator-on orientation. This Figure shows however, the existence of a fraction of stars with \mathcal{V}_{eq} velocities larger than the corresponding $v \sin i$ values. In other words, the projected observed $v \sin i$ velocities underestimate the real \mathcal{V}_{eq} velocities. Because stellar radii are fixed, this means that some stars are rotating faster due to smaller periods, than would be indicated by the $v \sin i$ values.

In Figure 6 we present a different type of representation that help us to distinguish among the faster rotators, which types of stars deplete their Li more rapidly. In this Figure the estimated stellar radii taken from Messina et al. (2010) for associations ABDA, THA, COA and CAA are presented against the projected $v \sin i$ observed values. For larger values of $v \sin i$ (equivalent to real larger \mathcal{V}_{eq} values) the corresponding stellar radii are between 0.8 and $1.0 R_{\odot}$, which represents well the K-type dwarf stars radii values. These stars normally deplete their Li faster than FG-type stars in the rapid rotators zone due to their larger CZ.

4. On the lithium desert

The existence of a specific and a relatively small region in the general $A(\text{Li})-T_{\text{eff}}$ stellar map, apparently devoid of field stars, was proposed by Ramírez, et al. (2012) (thereafter RA12) and was called the “lithium desert”, defined by the interval $5950 < T_{\text{eff}} < 6100 \text{ K}$ and $1.55 < A(\text{Li}) < 2.05$. The existence of such a region was inspired by the work of Chen, et al. (2001), which found an empty area centered at $A(\text{Li}) \sim 1.5$. This zone was separated by a bi-modal distribution of Li-rich and Li-poor stars. They considered that due to a strong correlation found among low Li stars of the Li Dip stars between mass and $[\text{Fe}/\text{H}]$ by Chen, et al. (2001) that could also be the case in the low Li side of the empty area. In this sense, according to this, the low Li side could contain evolved Li dip stars.

This apparent connection with Li dip stars was discussed in RA12, indicating that a relation between mass and $[Fe/H]$ in the higher Li side also exists, and this was found using the same data of Chen, et al. (2001). At the same time RA12 found, this time using their own data, that a similar mass-metallicity relation exists in the lower Li zone, but with a somewhat larger dispersion. All these properties led RA12 to consider that the contribution of evolved Li dip stars might not be important.

Nevertheless, the main problem that appeared consisted on answering the question of what causes this Li desert. A process of rapid and not yet identified Li depletion mechanism could then exist in order to explain the complete absence of stars in this intermediate void region. A more recent research by Aguilera-Gómez, Ramírez & Chanamé (2018) (hereafter AG18) using twice the number of stars in RA12, studied in detail the problem of the lithium desert. They proposed that both scenarios (evolved Li Dip population and a severely Li depleted zone) were partially correct. In any case, in both works (RA12 and AG18), the problem on how to explain the physical reason of this apparent absence of stars in the Li desert remained. We note, however, that AG18 found two apparently normal stars (one without planets, HD 90422, and another with planets, HD 31253) located in the box of the Li desert.

Not only AG18, but there are other authors who have found the presence of stars inside that box, for example López-Valdivia et al. (2015), who detected three stars inside the lithium desert: BD+47, HD 44985 and #58440 of the OC M4 ([MVB2012] 58440). Consequently, it seems that the Li desert is not completely empty of stars. In fact this hypothesis became a reality, because as a result, we identify that several stars could be present in a box (hereafter Box) corresponding to the Li desert. We detect some “new” stars belonging to the Box by the means of the use of new T_{eff} values furnished by space observatories as *Gaia*.

In a certain way, this is a challenging problem due to the reduced size of this Box, meaning that sufficiently reliable T_{eff} values must be used in order to know if a star belongs to the Box or not. In this analysis we only consider stars with a mean uncertainty less or equal of ± 0.1 for the $A(\text{Li})$ and 150 K for the effective temperatures. For this, we calculated the average between the maximum and minimum values of temperature, this is $(B_{T_{\text{eff}}} - b_{T_{\text{eff}}})/2$ using the uncertainties given by *Gaia* as described in Section 2. Let us remark that the value of an error of 150 K is near the size in T_{eff} of the Box. Diving into the *Gaia* DR2 catalogue, which has a large variety of T_{eff} errors for individual stars, we found several candidates that are considered as the basis of our approach.

We detect 13 stars in the Box with a mean uncertainty in T_{eff} of less than 150 K. Due to these uncertainties, several of them can stay in or out of the Box. In fact we detected 17 stars outside the Box, but due to their individual T_{eff} uncertainties (150 K), could get into the Box (see Table 3). We refer these stars as “near-Box” in the last column of Table 3. From the total 30 stars that can participate in this enter-exit balance, there are 24 stars without detected planets and six planetary host stars. We note that these detected mentioned 17 stars out of the Box are all stars with T_{eff} values smaller than the cool limit T_{eff} of the Box, i.e., $T_{\text{eff}} = 5950$ K.

We also explore for eventual candidates that could enter into the Box with values larger than the hot limit of $T_{\text{eff}} = 6100$ K. We found seven candidates up to maximum values of T_{eff} near 6300 K. Nevertheless, all of them have mean uncertainties in T_{eff} larger than 150 K, then do not fulfill the conditions to enter into the Box in this analysis.

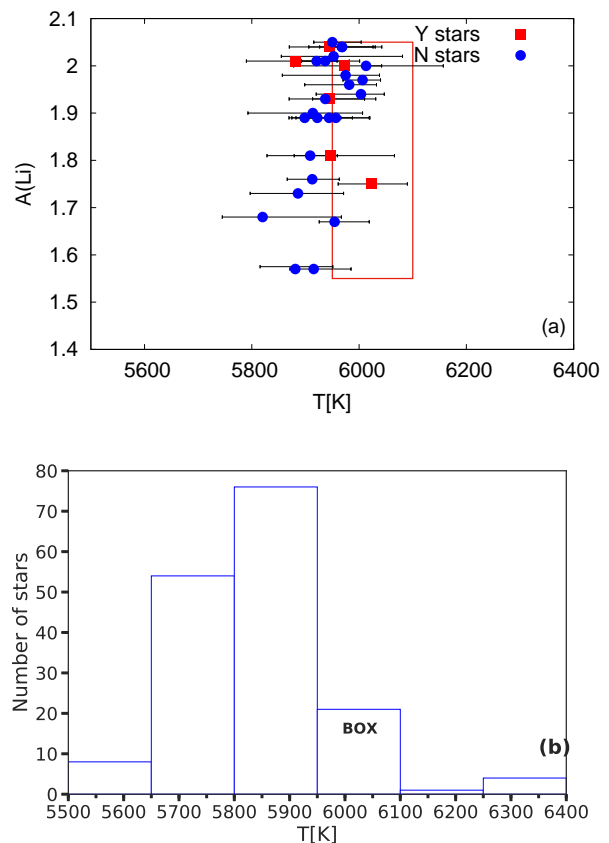


Fig. 7. (a) $A(\text{Li})$ distribution versus T_{eff} for the 30 stars in a near region of the “lithium desert” as defined by RA12, and represented by the green square called Box. Stars without detected planets (N) and stars host of planets (Y) are represented by blue filled circles and red filled squares. (b) Distribution in T_{eff} of the number of stars in six comparative boxes around the Box for the limits $1.55 < A(\text{Li}) < 2.05$. The bar with the label “Box” represents the green square of Figure (a) corresponding to the region of the called lithium desert.

When we analyse the two stars lying in the Box detected by AG18 by means of *Gaia* DR2 T_{eff} we obtain the next: the planet host star HD 31253 (◐) remains in all cases inside the Box, whereas the non-planetary host star HD 90422 could go out from the Box taking into account the uncertainties (see Table 1).

Figure 7a shows the distribution of the stars in the defined Box in the plane $A(\text{Li})$ - T_{eff} within the error limit for the effective temperatures. It is found a proportion of six host planet stars against 24 non-planet host, is this a typical representative value? The answer is yes, because this rate of 0.25 (6/24) is the same ratio that we found when considering the ~ 250 host planet stars in our whole catalogue divided by the approximate value of 1070 non-planet host stars. By considering the uncertainties in T_{eff} , more stars can enter in the Box than those that can leave it.

Figure 7b presents a histogram of effective temperature of the stars of the sample (Table 1) with $1.55 < A(\text{Li}) < 2.05$. This is the same range in lithium abundance of the Box. For reasons of homogeneity in the comparison with the other stars in the field, the called Box in the histogram of Figure 7b, contain a number of stars corresponding to the full sample, this is regardless the errors in T_{eff} . For this reason, in the bin corresponding to the Box appear more stars than those in Figure 7a. It is clear in this histogram how the density of stars varies according to the range of temperature considered, dropping considerably in the called Box, which is indicated in the corresponding bar. In Figure 8

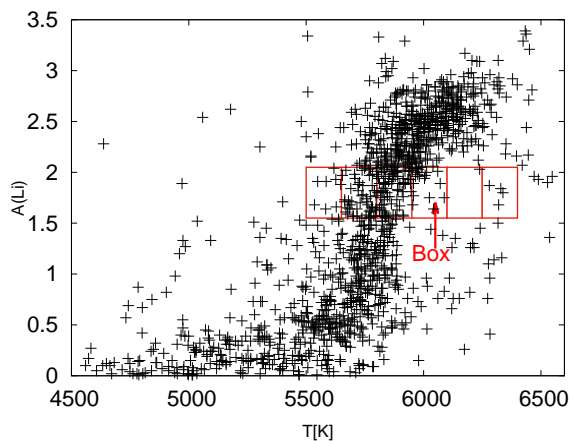


Fig. 8. $A(\text{Li})$ distribution versus T_{eff} for all the sample of Table 1. Six comparative boxes of Figure 7b indicating the variations of the number of stars are superposed to the Figure. An arrow is drawn to show the location of the box corresponding with the lithium desert.

Table 3. Parameter of stars in or near the Box of the “lithium desert”

Star	T_{eff} (K)	$b_{-}T_{\text{eff}}$ (K)	$B_{+}T_{\text{eff}}$ (K)	$A(\text{Li})$	Planet	Located
HD208	6013	5865	6157	2.00 ± 0.10	N	Box
HD7134	5975	5858	6038	1.98 ± 0.10	N	Box
HD31253	6025	5961	6090	1.75 ± 0.02	Y	Box
HD36108	5982	5899	6033	1.96 ± 0.02	N	Box
HD38510	5952	5855	6081	2.02 ± 0.02	N	Box
HD83529	6004	5920	6048	1.94 ± 0.02	N	Box
HD86081	5973	5878	6042	2.00 ± 0.08	Y	Box
HD90081	6007	5970	6040	1.97 ± 0.10	N	Box
HD110897	5968	5927	6026	2.04 ± 0.11	N	Box
HD153627	5954	5926	6020	1.68 ± 0.02	N	Box
HD165499	5950	5916	6005	2.05 ± 0.10	N	Box
HD193193	5968	5906	6042	2.04 ± 0.02	N	Box
HD201496	5957	5875	6019	1.89 ± 0.15	N	Box
HD16382	5937	5893	5982	2.01 ± 0.10	N	Near-Box
HD17865	5886	5797	5971	1.73 ± 0.12	N	Near-Box
HD20407	5909	5879	5960	1.81 ± 0.12	N	Near-Box
HD31527	5922	5905	5988	1.89 ± 0.02	N	Near-Box
HD55575	5913	5866	5964	1.76 ± 0.10	N	Near-Box
HD74957	5899	5882	5966	1.89 ± 0.10	N	Near-Box
HD95128	5947	5828	6066	1.81 ± 0.04	Y	Near-Box
HD97037	5881	5816	5950	1.57 ± 0.02	N	Near-Box
HD114762	5946	5870	6030	$2.04 \pm -$	Y	Near-Box
HD117105	5937	5870	6031	1.93 ± 0.03	N	Near-Box
HD119173	5914	5793	6007	1.90 ± 0.12	N	Near-Box
HD141624	5915	5871	5985	1.57 ± 0.15	N	Near-Box
HD147513	5883	5790	5959	2.01 ± 0.02	Y	Near-Box
HD148816	5944	5869	6021	1.89 ± 0.02	N	Near-Box
HD198089	5820	5746	5967	1.68 ± 0.05	N	Near-Box
HD199289	5921	5885	6001	2.01 ± 0.10	N	Near-Box
HD220689	5944	5913	6011	1.93 ± 0.02	Y	Near-Box

References.

Col.1: Henry-Draper catalog name; Col.2-3-4: effective temperature taken from *Gaia* DR2 and their lower ($b_{-}T_{\text{eff}}$) and upper limit ($B_{+}T_{\text{eff}}$); Col.5: Lithium abundance; Col.6: presence of planets Yes or No, and Col.7: location in or near the Box.

we show the whole map of $A(\text{Li})$ against T_{eff} (*Gaia*) of field stars of Table 1. The six comparative boxes of the histogram used to see the variations of the number of stars around the Box are superimposed to the Figure. From this point of view the “lithium desert” appears not to be a real problem but more, a statistical distribution fluctuation.

5. Discussion and Conclusions

This paper covers two different topics. One, in Section 3, is devoted to the lithium-rotation connection (LRC) for stars with masses between $0.8 M_{\odot}$ and $1.4 M_{\odot}$ and stellar types from F5 up to K4. The most important manifestation of the LRC being that for very low stellar rotations, stars appear to be in general Li-poor whereas they appear Li-rich for larger rotations. The second topic (Section 4) refers to the existence or not, of what is known in the literature as the “lithium desert” appearing in the general distribution of the lithium abundance $A(\text{Li})$ of these stars in function of effective temperatures T_{eff} (Figure 2).

We summarise what we have learned over this study of the lithium rotation connection. The first new result consists of an observational determination of a critical threshold of projected rotational velocity $v \sin i$ value which separates slow and high stellar rotators. For this purpose we used in Section 3 a general distribution of the Li abundance values of field stars, with and without planets, in function of the T_{eff} *Gaia* values (Figure 2). To this distribution we added a third parameter; their corresponding $v \sin i$ values. However, this Figure does not allow us to obtain a robust indication of this threshold velocity. A more detailed approach was then necessary to better determine this critical velocity. This was done by means of the distribution of Li abundance values versus the $v \sin i$ values adding a third axis representing other stellar parameters; that is depicted in a mosaic shown in Figure 3.

A more realistic critical rotation velocity was found. After our analysis we conclude that those stars with $v \sin i < 5 \text{ km s}^{-1}$ (slow rotators) have different properties of age and T_{eff} (especially in this one) than those stars with $v \sin i > 5 \text{ km s}^{-1}$ (fast rotators), either for field stars with or without planets or cluster stars. In short, the critical projected rotational velocity can be considered represented by the value of 5 km s^{-1} . This critical rotational velocity is representative of the lithium-rotation connection, moreover also separates other physical parameters.

This critical velocity is important for models that study the LRC as is the case of the Li depletion hydrodynamic model of Baraffe, et al. (2017). In this model, this critical velocity separates the effects of penetrating plumes at the lower edge of the convection internal zone producing the Li depletion. We should stress here, that we also explored independently, from our data described in Section 2, two relevant catalogues of $A(\text{Li})$. First, the AMBRE/Li catalogue of Guiglion et al. (2016), which was filtered from repeated values and other inconsistencies. We finally found for this catalogue 4927 clean actual star members of which only 2300 are dwarf FGK stars. In fact, Guiglion et al. (2016) recognise a subsample of 2310 dwarf stars. A detailed discussion of this filtering process will be given in our next work of these series. The second catalogue was published by Bensby & Lind (2018) which contains 515 stars. We searched, for both catalogues, the projected rotational velocities in the literature with the same tool as described in Section 2. In both samples, we found approximately the same threshold critical velocities as mentioned above.

Regarding our study on the age dependency of the LRC properties, we summarise the knowledge on this subject. As mentioned in the Introduction, Bouvier et al. (2016) have detected the presence of the LRC in a very young open cluster of 5 Myr (NGC 2264). It is interesting to note that this age corresponds to the PMS stage, suggesting this way, a relation of the LRC with the very initial stellar stages of the lives of low-mass stars. In NGC 2264, the LRC is acting on stars with masses in the interval $0.5\text{--}1.2 M_{\odot}$, which is relatively similar to the interval of masses

considered here ($0.8\text{--}1.4 M_{\odot}$). For larger ages, Messina et al. (2016) detected the action of the LRC in the Beta Pic association (20 Myr) but only, in a clear way, for very low mass stars between $0.3 M_{\odot}$ and $0.8 M_{\odot}$. For stars with masses larger than $0.8 M_{\odot}$ the LRC appears only to be incipient in this association. Several doubts arose when explaining this different behaviour, but we note that both groups are in the general poorly known spin up stage for low mass stars, that finish at $\sim 30\text{--}40$ Myr (Bouvier et al. 2014). The next age step of the LRC studied in the literature is that of the open cluster Pleiades (125 Myr) and on the stellar stream Pec-Eri, with a similar age as the Pleiades. Our contribution on the age dependency study of LRC, refers to the second and final general rotation stage, the spin down, also beginning at $\sim 30\text{--}40$ Myr and lasting forever (Bouvier et al. 2014).

For all the stellar associations studied here, we first detected and eliminated all intruder members. To do this we employed a simple chemical method by which we considered as an intruder any star member that had an individual metallicity value quite different from the mean group metallicity. For this purpose we determined these new mean group metallicities for four associations (see Section 3.2) for which only one metallicity association value appears in the literature. Also, considering that the associations Tucana-Horologium, Columbus and Carina have a similar age of 45 Myr, this signifies that they are just at the beginning of this general rotational braking stage. In Figure 4 we show the behaviour of $A(\text{Li})$ versus $v \sin i$ for these three associations with their genuine stellar components, where intruder members were eliminated. In this Figure, a typical pattern appear in which Li depleted stars are present for $v \sin i$ values less than a critical $v \sin i < 10 \text{ km s}^{-1}$ value.

For $v \sin i$ values larger than this critical velocity, a single branch of inhibited Li depletion stars appears. This branch continues up to very large rotational values. However, a minimum Li depletion characteristic of these young associations, appears at $v \sin i \sim 50 \text{ km s}^{-1}$. This kind of pattern is important, because in the next studied association, AB Doradus (ABDA), an extra branch of strong Li depletion appears, beginning at $v \sin i \sim 30 \text{ km s}^{-1}$ and continues up to large rotation values of $\sim 70 \text{ km s}^{-1}$ as it is seen in Figure 5a. This new branch of very strong Li depletion, is formed by low-mass K-dwarfs and their rapid Li depletion acts together according to their minimal masses. This behaviour of K-type dwarfs is in agreement with the distribution of their stellar radii with $v \sin i$ as shown in Figure 6. The other branch composed essentially by only three stars of FGK-types, follows the same pattern as is the case of the stellar groups at 45 Myr, attaining very large rotations, larger than $\sim 130 \text{ km s}^{-1}$. But even in this case, the only very high rapid K-dwarf rotator at $v \sin i = 140 \text{ km s}^{-1}$, is the only one that depletes Li. Let us note that this double branch depletion pattern in ABDA, it is also found in the Pleiades (see Figure 5b). This similarity agrees with the fact that both, the ABDA and the Pleiades, have not also the same age around 120 Myr but also that both stellar groups have a common origin (Ortega et al. 2007).

We understand that the formation of a second depletion branch in groups at 120 Myr, is a consequence of the general diminishing of stellar rotation for that age, during the general spin down era. We remark that the birth of the first depletion branch in ABDA at $v \sin i \sim 30 \text{ km s}^{-1}$, corresponds also to the minimum Li depletion of the Pleiades as it is seen in Figure 5. This value is smaller than the value of $v \sin i \sim 50 \text{ km s}^{-1}$ of the mentioned minimum Li depletion in the younger associations. We note, however, that for the open cluster Alpha Per with an age of (50-70 Myr) which is relatively intermediate be-

tween of our considered younger associations (45 Myr) and that of ABDA (120 Myr), the Li minimum also appears at $v \sin i = 50 \text{ km s}^{-1}$ but even more, at this velocity a double branch is formed similarly as is the case of ABDA (see Figure 3 in Balachandran, Lambert, & Stauffer 1988). In this Figure it can be seen that the LRC pattern in Alpha Per, at this intermediate age, shows a mixture of properties between the associations at 45 Myr and 120 Myr mentioned before.

To explore the behaviour of the LRC for larger ages, we considered the open cluster NGC 1039 with an age of 250 Myr. Following the classical publication of this cluster by Jones et al. (1997), we plot the $A(\text{Li})$ versus $v \sin i$ values (plot not shown in this paper) for members with more than 75% member probability. The corresponding minimum of Li depletion corresponds to near 17 km/s . Separately, we confirmed this same value of $\sim 17 \text{ km s}^{-1}$, by plotting for members of NGC 1039 with more than 90% member probability, by using the $A(\text{Li})$ values of Sestito & Randich (2005) and $v \sin i$ values compiled and described in Section 2. We conclude that in a period going from the age of 45 Myr of the younger associations considered here, up to the age of 250 Myr of NGC 1039, (i.e. a 200 Myr interval), their minimum Li depletion points have shifted from the corresponding $v \sin i$ value of $\sim 50 \text{ km s}^{-1}$ at 45 Myr to somewhat less than 20 km s^{-1} for 250 Myr. This shift appears also to be a direct consequence of the general spin down of the stars rotation behaviour. Other conclusion of this work, is that K-dwarf stars are the first to deplete their Li in these early stages in the main-sequence at large rotation velocities, due to their important convective zones. This behaviour is also due to the general spin down of low mass stars. We can try to quantify this behaviour by estimating the mean $v \sin i$ values for our studied stellar moving groups with ages at 45 Myr and 120 Myr. These approximate mean values of $v \sin i$ are respectively equal to 32 km s^{-1} and 20 km s^{-1} . Their ratio $32/20 = 1.6$ can be compared with that expected in the general theoretical braking rotational curves, for slow and fast rotators (see Figure 7 in Bouvier et al. 2014). For these ages, the ratios are 1.6 and ~ 2.0 respectively, which is in agreement with the observed values of our chosen associations.

Section 4 was devoted entirely to the study of what was considered in the literature as the ‘‘lithium desert’’. In a first sight, this region shows an anomalous absence of stars which also presented an unsolved problem, regarding as which is the physical mechanism that provokes such a radical Li depletion. In reality, by means of new T_{eff} values obtained from *Gaia* DR2, we found that the ‘‘lithium desert’’ appears to be a false problem as we detected in this work 30 stars that are in the box defined above or very near to it. Due to the uncertainties of the *Gaia* T_{eff} values, from these 30 objects, 13 stars in the box can remain or leave the box and nearby 17 stars can enter into the box. In any case, the box representing the ‘‘lithium desert’’ probable contain stars. A population test was made to see if a possible inference of the actual number of stars of the Box is reasonable. All this in comparison with the whole nearby stars population in that $A(\text{Li})$ interval. We found that approximately 15 stars can occupy the region of what was called the ‘‘lithium desert’’. This shows that the considered past absence of stars was more likely a result of an statistical fluctuation distribution effect.

Acknowledgements

The authors thank the anonymous referee for the constructive comments and helpful insights. This work has made use of SVODiscTool, developed by the Spanish Virtual Observatory (Centro de Astrobiología (CSIC-INTA), Unidad de Exce-

lencia María de Maeztu), a project supported by the Spanish State Research Agency (AEI) through grants AyA2017-84089 and MDM-2017-0737. C.CH acknowledges support from SE-CYT/UNC and CONICET. FLA and R de la R. acknowledge support from the Faculty of the European Space Astronomy Centre (ESAC) - Funding references 569 and 570, respectively. FLA would like to thank the technical support provided by A. Parras (CAB), Dr. J. A. Prieto (UCLM) and MSc J. Gómez Malagón. Authors also thank to Leo Girardi for providing the PARAM code. SFR acknowledges support from a Spanish post-doctoral fellowship ‘Ayudas para la atracción del talento investigador. Modalidad 2: jóvenes investigadores, financiadas por la Comunidad de Madrid’ under grant number 2017- T2/TIC-5592. SRF acknowledges financial support from the Spanish Ministry of Economy and Competitiveness (MINECO) under grant number AYA2016-75808-R, AYA2017-90589-REDT and S2018/NMT-429, and from the CAM-UCM under grant number PR65/19-22462 and from the CAM-UCM under grant number PR65/19-22462. CC acknowledges financial support from the Spanish Ministry of Science and Innovation through grants AYA2016-79425- C3-1/2/3-P and BES-2017-080769

References

- Aguilera-Gómez C., Ramírez I., Chanamé J., 2018, *A&A*, 614, A55
- Ahrens B., Stix M., Thorn M., 1992, *A&A*, 264, 673
- Andrae R., et al., 2018, *A&A*, 616, A8
- Anthony-Twarog B. J., Deliyannis C. P., Twarog B. A., Croxall K. V., Cummings J. D., 2009, *AJ*, 138, 1171
- Anthony-Twarog B. J., Deliyannis C. P., Rich E., Twarog B. A., 2013, *ApJL*, 767, L19
- Arancibia J., Bouvier J., Bayo A., Galli P. A. B., Brandner W., Bouy H., Barrado D., 2020, *BAAA*, 61R, 61C, 81
- Armitage P. J., Clarke C. J., Palla F., 2003, *MNRAS*, 342, 1139. doi:10.1046/j.1365-8711.2003.06604
- Asplund M., Grevesse N., Sauval A. J., Scott P., 2009, *ARA&A*, 47, 481. doi:10.1146/annurev.astro.46.060407.145222
- Balachandran S., Lambert D. L., Stauffer J. R., 1988, *ApJ*, 333, 267. doi:10.1086/166743
- Baraffe I., et al., 2017, *ApJL*, 845, L6
- Barenfeld S. A., Bubar E. J., Mamajek E. E., Young P. A., 2013, *ApJ*, 766, 6. doi:10.1088/0004-637X/766/1/6
- Barrado D., Bouy H., Bouvier J., Moraux E., Sarro L. M., Bertin E., Cuillandre J.-C., et al., 2016, *A&A*, 596, A113. doi:10.1051/0004-6361/201629103
- Baugh P., King J. R., Deliyannis C. P., Boesgaard A. M., 2013, *PASP*, 125, 753. doi:10.1086/671721
- Bell C. P. M., Mamajek E. E., Naylor T., 2015, *MNRAS*, 454, 593. doi:10.1093/mnras/stv1981
- Bensby T., Lind K., 2018, *A&A*, 615, A151
- Bouvier J., Matt S. P., Mohanty S., Scholz A., Stassun K. G., Zanni C., 2014, *prpl.conf*, 433. doi:10.2458/zu-uapress-9780816531240-ch019
- Bouvier J., Lanzafame A. C., Venuti L., Klutsch A., Jeffries R., Frasca A., Moraux E., et al., 2016, *A&A*, 590, A78. doi:10.1051/0004-6361/201628336
- Bouvier J., Barrado D., Moraux E., Stauffer J., Rebull L., Hillenbrand L., Bayo A., et al., 2018, *A&A*, 613, A63. doi:10.1051/0004-6361/201731881
- Bouvier J., 2020, *arXiv*, arXiv:2009.02086
- Boro Saikia, S., Marvin, C. J., Jeffers, S. V., et al. 2018, *A&A*, 616, A108
- Brewer J. M., Fischer D. A., Valenti J. A., Piskunov N., 2016, *yCat*, J/ApJS/225/32
- Brown D. J. A., Collier Cameron A., Hall C., Hebb L., Smalley B., 2011, *MNRAS*, 415, 605
- Butler R. P., Cohen R. D., Duncan D. K., Marcy G. W., 1987, *ApJL*, 319, L19. doi:10.1086/184947
- Chavero C., de la Reza R., Ghezzi L., Llorente de Andrés F., Pereira C. B., Giuppone C., Pinzón G., 2019, *MNRAS*, 487, 3162
- Chen Y. Q., Nissen P. E., Benoni T., Zhao G., 2001, *A&A*, 371, 943
- Conti P. S., 1968, *ApJ*, 152, 657. doi:10.1086/149581
- Cummings J. D., Deliyannis C. P., Anthony-Twarog B., Twarog B., Maderak R. M., 2012, *AJ*, 144, 137
- Cutispoto G., Pastori L., Pasquini L., de Medeiros J. R., Tagliaferri G., Andersen J., 2002, *yCat*, J/A+A/384/491
- da Silva L., et al., 2006, *A&A*, 458, 609
- da Silva L., Torres C. A. O., de La Reza R., Quast G. R., Melo C. H. F., Sterzik M. F., 2009, *A&A*, 508, 833
- da Silva Santos J. M., de la Cruz Rodríguez J., Leenaarts J., Chintzoglou G., De Pontieu B., Wedemeyer S., Szydlarski M., 2020, *A&A*, 634, A56
- Deal M., Richard O., Vauclair S., 2015, *A&A*, 584, A105
- Delgado Mena E., et al., 2014, *yCat*, J/A+A/562/A92
- Delgado Mena E., et al., 2015, *yCat*, J/A+A/576/A69
- Delgado Mena E., et al., 2019, *A&A*, 624, A78
- Dias W. S., Monteiro H., Caetano T. C., Lépine J. R. D., Assafin M., Oliveira A. F., 2014, *A&A*, 564, A79. doi:10.1051/0004-6361/201323226
- Dias W. S., Alessi B. S., Moitinho A., Lepine J. R. D., 2014, *yCat*, B/ocl
- Duchêne G., 2010, *ApJL*, 709, L114
- Dumont T., Palacios A., Charbonnel C., Richard O., Amard L., Augustson K., Mathis S., 2020, *arXiv*, arXiv:2012.03647
- Eggenberger P., Haemmerlé L., Meynet G., Maeder A., 2012, *A&A*, 539, A70
- Ford E. B., Rasio F. A., 2006, *ApJL*, 638, L45
- Gaia Collaboration, et al., 2016, *A&A*, 595, A1
- Gaia Collaboration, Brown, A. G. A., Vallenari, A., et al. 2018, *A&A*, 616, A1
- García Villota A., 2021, *MST*, Universidad Nacional de Colombia
- Gaspar A., Rieke G. H., Ballering N., 2016, *yCat*, J/ApJ/826/171
- Gáspár, A., Rieke, G. H., & Ballering, N. 2016, *ApJ*, 826, 171
- Ghezzi L., Cunha K., Smith V. V., de la Reza R., 2010, *ApJ*, 724, 154
- Glebocki R., Gnacinski P., 2005, *yCat*, III/244
- Gonzalez G., Carlson M. K., Tobin R. W., 2010, *MNRAS*, 403, 1368
- Gonzalez G., 2015, *MNRAS*, 446, 1020
- Guiglion G., de Laverny P., Recio-Blanco A., Worley C. C., De Pascale M., Masseron T., Prantzos N., et al., 2016, *A&A*, 595, A18. doi:10.1051/0004-6361/201628919
- Guiglion G., et al., 2019, *A&A*, 623, A99
- Helmi A., Babusiaux C., Koppelman H. H., Massari D., Veljanoski J., Brown A. G. A., 2018, *Nature*, 563, 85
- Heiter U., Soubiran C., Netopil M., Paurzen E., 2014, *A&A*, 561, A93. doi:10.1051/0004-6361/201322559
- Herbig G. H., 1966, *AnAp*, 29, 593
- Ireland L. G., Zanni C., Matt S. P., Pantolmos G., 2021, *csss.conf*, 163. doi:10.5281/zenodo.4565111
- Israelian G., Santos N. C., Mayor M., Rebolo R., 2004, *A&A*, 414, 601
- Jeffries R. D., Jackson R. J., Deliyannis C. P., Sun Q., 2020, *MmSAI*, 91, 88
- Jones B. F., Fischer D., Shetrone M., Soderblom D. R., 1997, *AJ*, 114, 352. doi:10.1086/118479
- Kharchenko N. V., Piskunov A. E., Roeser S., Schilbach E., Scholz R.-D., 2005, *yCat*, J/A+A/438/1163
- Kharchenko N. V., Piskunov A. E., Roeser S., Schilbach E., Scholz R.-D., 2013, *yCat*, J/A+A/558/A53
- King J. R., Krishnamurthi A., Pinsonneault M. H., 2000, *AJ*, 119, 859. doi:10.1086/301205
- Krejčová, T., & Budaj, J. 2012, *A&A*, 540, A82
- Lambert D. L., Reddy B. E., 2004, *MNRAS*, 349, 757. doi:10.1111/j.1365-2966.2004.07557.x
- Lodders K., Palme H., Gail H.-P., 2009, *LanB..4B*, 4B, 712. doi:10.1007/978-3-540-88055-4-34
- López-Valdivia R., Hernández-Águila J. B., Bertone E., Chávez M., Cruz-Saenz de Miera F., Amazo-Gómez E. M., 2015, *MNRAS*, 451, 4368
- Luck R. E., 2017, *yCat*, J/AJ/153/21
- Lyubimkov L. S., 2016, *Ap*, 59, 411. doi:10.1007/s10511-016-9446-5
- Luhman K. L., Stauffer J. R., Mamajek E. E., 2005, *ApJL*, 628, L69. doi:10.1086/432617
- Lyubimkov L. S., 2018, *Ap*, 61, 262
- Marsden S. C., et al., 2014, *MNRAS*, 444, 3517
- Messina S., Lanzafame A. C., Feiden G. A., Millward M., Desidera S., Buccino A., Curtis I., et al., 2016, *A&A*, 596, A29. doi:10.1051/0004-6361/201628524
- Messina S., Desidera S., Turatto M., Lanzafame A. C., Guinan E. F., 2010, *A&A*, 520, A15. doi:10.1051/0004-6361/200913644
- Michaud G., Charbonneau P., 1991, *SSRv*, 57, 1
- Mor R., Robin A. C., Figueras F., Roca-Fàbrega S., Luri X., 2019, *A&A*, 624, L1
- Müller E. A., Peytremann E., de La Reza R., 1975, *SoPh*, 41, 53
- Pinheiro F. J. G., et al., 2014, *MNRAS*, 445, 2223
- Ortega V. G., Jilinski E., de La Reza R., Bazzanella B., 2007, *MNRAS*, 377, 441. doi:10.1111/j.1365-2966.2007.11614.x
- Ramírez I., Fish J. R., Lambert D. L., Allende Prieto C., 2012, *ApJ*, 756, 46
- Rüdiger G., Pipin V. V., 2001, *A&A*, 375, 149
- Tschäpe R., Rüdiger G., 2001, *A&A*, 377, 84. doi:10.1051/0004-6361:20010482
- Sestito P., Randich S., 2005, *A&A*, 442, 615
- Siess L., Livio M., 1997, *ApJ*, 490, 785. doi:10.1086/304905
- Somers G., Pinsonneault M. H., 2014, *ApJ*, 790, 72. doi:10.1088/0004-637X/790/1/72
- Somers G., Stassun K. G., 2017, *AJ*, 153, 101. doi:10.3847/1538-3881/153/3/101

- Soderblom D. R., Jones B. F., Balachandran S., Stauffer J. R., Duncan D. K., Fedele S. B., Hudon J. D., 1993, *AJ*, 106, 1059. doi:10.1086/116704
- Soubiran, C., Le Campion, J.-F., Brouillet, N., et al. 2016, *A&A*, 591, A118
- Soubiran F., Militzer B., 2016, *yCat*, J/ApJ/829/14
- Stephens A., Boesgaard A. M., King J. R., Deliyannis C. P., 1997, *ApJ*, 491, 339
- Takeda Y., Kawanomoto S., 2005, *PASJ*, 57, 45
- Thevenin F., 1998, *yCat*, III/193
- Torres C. A. O., da Silva L., Quast G. R., de la Reza R., Jilinski E., 2000, *AJ*, 120, 1410. doi:10.1086/301539
- Torres C. A. O., Quast G. R., Melo C. H. F., Sterzik M. F., 2008, *hsf2.book*, 757
- Zuckerman B., Webb R. A., 2000, *ApJ*, 535, 959. doi:10.1086/308897
- Zuckerman B., Song I., Bessell M. S., 2004, *ApJL*, 613, L65. doi:10.1086/425036

